**NURETH14-562** 

# TRIO\_U ANALYSIS OF NATURAL CONVECTION IN THE UPPER PLENUM OF THE MONJU REACTOR

U. Bieder<sup>1</sup>, G. Fauchet<sup>1</sup> and S. Yoshikawa<sup>2</sup>
<sup>1</sup>CEA, DEN, DER/SSTH, Grenoble, France
<sup>2</sup>JAEA, Tsuruga, Japan

#### **Abstract**

The IAEA is coordinating a benchmark project on natural convection phenomena in the Upper Plenum of the MONJU reactor. The JAEA has provided both detailed geometrical data of the plant and complete thermalhydraulic boundary conditions describing a pump trip transient, accomplished during the start-up experiments. For the initial conditions of the pump trip transient, extensive sensitivity analyses have been made with the CFD code Trio\_U. These calculations show a high sensitivity of the global flow pattern in the MONJU Upper Plenum depending on the order of the numerical scheme and the modeling of the geometrically complex Upper Core Structure. During the pump trip, the formation of a thermal stratification within the plenum has been observed which persists for more than one hour. All calculations with Trio\_U have shown a homogenization of the temperature in the plenum after about 15 minutes. A slight reduction of the mixing in the Upper Plenum could have been achieved by modifying the form of the flow holes in the Inner Barrel (fillets instead of sharp edges) in order to reduce their axial pressure loss.

## Introduction

The IAEA is coordinating a research project (CRP) entitled "Benchmark Analysis of Sodium Natural Convection in the Upper Plenum of the MONJU Reactor Vessel". JAEA has submitted to the CRP participants the data of sodium thermal stratification measurements in the in MONJU reactor vessel Upper Plenum collected during a plant trip test conducted in December 1995. The benchmark partners are analysing these experiment by applying different codes and methodologies. The benchmark will thus help the members to improve their capability in the field of fast reactor in-vessel sodium thermalhydraulics. The paper presents a numerical analysis of the pump trip experiment. The analysis has been carried out with the Trio\_U code. The calculations are compared to measurements taken along a thermocouple plug.

# 1. The MONJU plant

The Upper Plenum of the MONJU reactor is geometrically very complex. Figure 1 is a view of the complete Upper Plenum [1], [2]. The sodium flow is leaving the core through the Sub-Assemblies (SA) and is traversing the topologically very complex tube bundles of the Upper Core Structure (UCS) to enter the open space of the Upper Plenum. Then, the flow passes either above the Inner Barrel or passes through the flow holes of the Inner Barrel to reach the three outlet nozzles.

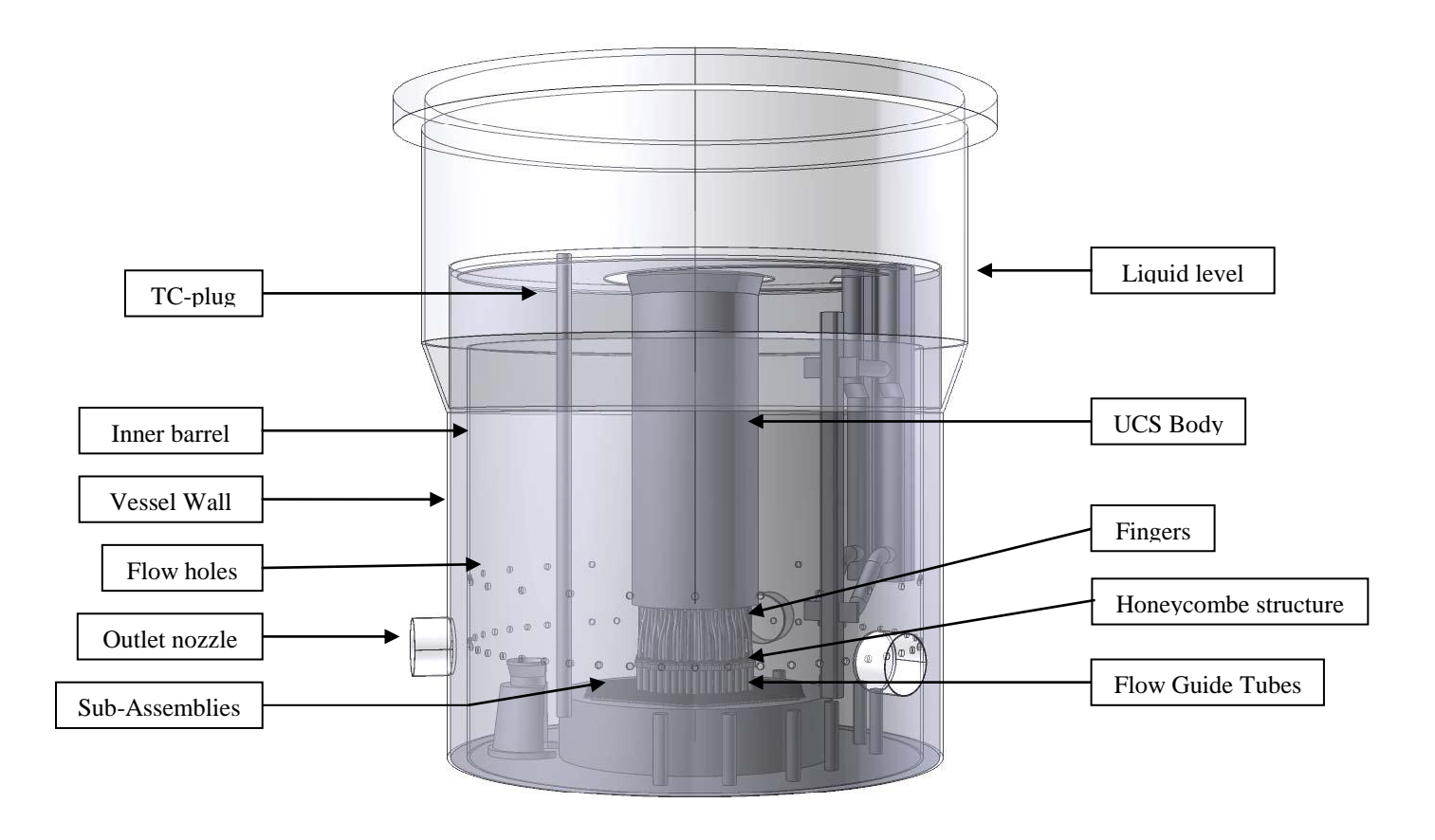


Figure 1 View of the complete Upper Plenum of the MONJU plant.

The Upper Core Structure is situated above the Sub-Assembly outlets and below the UCS-Body. This region is shown in more detail on Figure 2. The UCS can be divided into two regions:

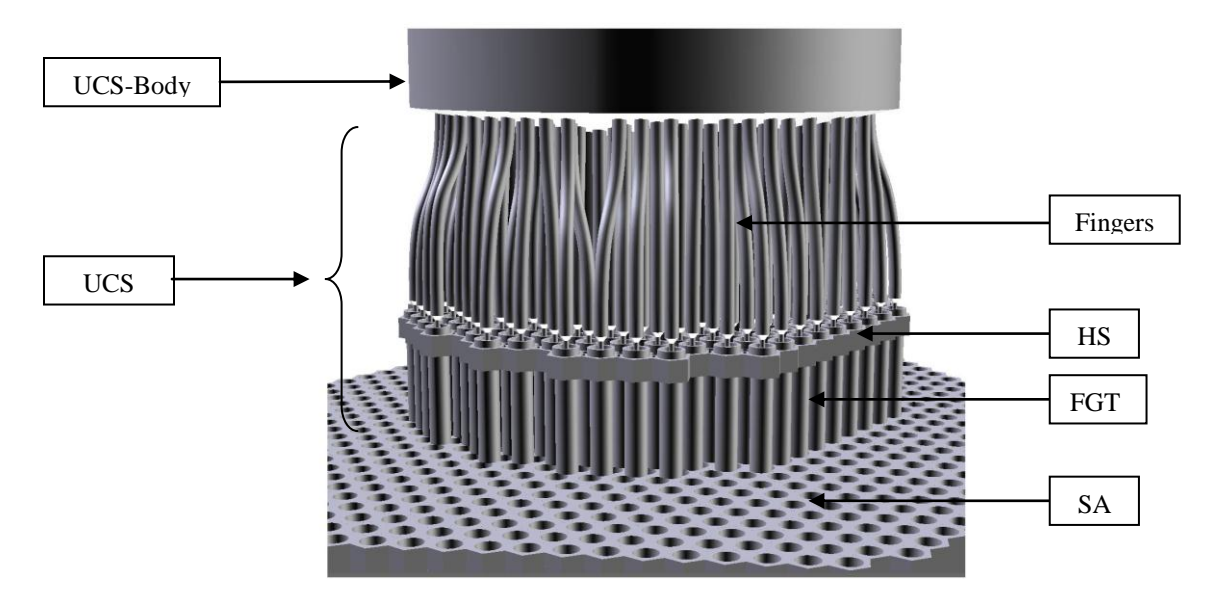


Figure 2 Zoom on the solid structures between core outlet and Upper Core Structure body

- The region of the Flow Guide Tubes (FGT) which is a tube bundle maintained at its top by a perforated plate called Honeycomb Structure (HS).
- The region of the Fingers located above the FGT and the HS.

The main flow passes inside the FGT to enter vertically the Fingers region. 19 Control Rod Guide Tubes are present inside both regions.

#### 2. Numerical model

# 2.1 The simplified geometry

A simplified CAD model has been developed at ANL [3] and consists of only 1/6 of the Upper Plenum of the MONJU reactor. A section of 60° is modelled where the following modifications have been made in order to obtain a symmetric geometry:

- All of the sub-assemblies outlets are taken as hexagonal,
- The top of the sub-assembly outlets are placed on different levels to distinct the different channels easily,
- The outlet nozzle is rotated to respect the hexagonal core configuration (only half of the outlet nozzle is modelled),
- The internal structures of the plenum like "In-Vessel Transfer Machine", "Lower Guide" or "Thermocouple plug" are not modelled.

Within the UCS, only the Control Rod Guide Tubes are realized in the CAD model. The FGT tubes as well as the Fingers are not treated explicitly due to their small size and geometrical complexity. However, the external frontiers of the FGT and Fingers regions are realized with the intention of forming in that way two sub-regions which allow a specific macroscopic modelling of the UCS.

# 2.2 Modelling the Upper Core Structure

In the presented approach, the UCS is modelled by a porous media with directional pressure losses [4]. The two regions (FGT and Fingers) are filled with tube bundles. The correlation defining the friction coefficient *Cf*, which is used to predict the pressure loss within these regions, is valid for flow inside and outside of tube bundles with a circular pitch [4]:

$$Cf = a \operatorname{Re}^{-b} \quad with \quad \operatorname{Re} = \frac{UD}{V}.$$
 (1)

Here, Re is the Reynolds number, U the local velocity, D a characteristic diameter and v the kinematic viscosity. The correlation distinguishes the axial and the transverse direction of the flow. The different parameters of the correlation are given in the Table 1.

Table 1 Parameters for the pressure loss correlation

	а	b	U	Characteristic diameter D
Axial direction	0.316	0.25	Axial velocity $\vec{U}_a$	Hydraulic diameter $D_h$
Transverse direction	4.03	0.27	Transverse velocity $\vec{U}_{\scriptscriptstyle t}$	External diameter of tubes $D_e$

A volumetric porosity of 0.83 is defined for the fingers region to simulate the acceleration of the flow outside of the tubes due to mass conservation considerations. The hydraulic diameter  $D_h$  is defined by:

$$D_h = \frac{4 S}{P}. \tag{2}$$

S is the fluid cross-section and P the wetted perimeter of the tubes. The axial velocity  $\vec{U}_a$  and transversal velocity  $\vec{U}_t$  is then calculated as a function of tube direction vector  $\vec{d}_a$ :

$$\vec{U}_a = (\vec{U}.\vec{d}_a) \vec{d}_a \quad and \quad \vec{U}_t = \vec{U} - \vec{U}_a. \tag{3}$$

The tube direction vector  $\vec{d}_a$  defines the main tube alignment and is simplified as the global vertical direction  $(0,0,1)^T$ . In CFD codes in general and in Trio\_U in particular, the directional pressure loss  $\vec{P}_L$  is treated as a source term in the Navier-Stokes equation. The parameters of the correlation for both regions are gathered in the Table 2.

Table 2 Pressure loss parameters

Table 2 Tressure Toss parameters					
	Type	Pressure loss correlation	Parameters		
FGT		$ ec{U} $ $ ec{U} $ $ ec{U} $	<i>D<sub>h</sub></i> =72 mm		
area		$\vec{P}_L = \frac{d\vec{U}}{dt} = -Cf_a \frac{ \vec{U}_a }{2.D_t} \vec{U}_a - Cf_t \frac{ \vec{U}_t }{2.D} \vec{U}_t$	$D_{ m e}$ =76 mm		
FGR area	Circular pitch bundle	$Cf_a = 0.316 \text{Re}^{-0.25}  \text{with}  \text{Re} = \frac{\left \vec{U}_a\right  D_h}{V}$ $Cf_t = 4.03 \text{Re}^{-0.27}  \text{with}  \text{Re} = \frac{\left \vec{U}_t\right  D_e}{V}$	$D_{h}=47.7 \text{ mm}$ $D_{e} = \begin{cases} 0.24m & for  EL \leq 27874 \\ 0.17m & for  EL \geq 28135 \\ linear \ between \ the \ two \ EL \end{cases}$		
		$Cf_t = 4.03 \text{ Re}^{-0.27}$ with $Re = \frac{1}{V}$	(unear between the two EL		

It is important to verify that the implementation of the transversal pressure loss leads to angle independent results for flow source in the centre of a symmetric rod bundle! The plate of the Honeycomb structure (HS) is modelled like a plate without any thickness. The singular pressure loss which is applied on the plate is a grid pressure loss correlation [4]. The directional pressure loss  $\Delta \vec{P}$  applied on the HS plate is defined as:

$$\Delta \vec{P} = \frac{1}{2} \rho K \left| \vec{U} \right| (\vec{U}.\vec{n}). \tag{4}$$

Here,  $\rho$  is the fluid density, K the pressure loss coefficient of the HS and  $\vec{n}$  the normal vector of the surface of the HS plate. According to [5], the value of the pressure loss coefficient K is constant during the trip test and is equal to 60.

# 2.3 Meshing

ANL has provided the CAD model of the simplified 60° geometry in IGES format. This model has been imported into the commercial mesh generator ICEMCFD. The UCS regions "FGT" and "Fingers" are defined as internal sub-domains and the Honeycomb structure is implemented as an internal, semi permeable wall. Two pure tetrahedral meshes of 300.000 elements (coarse mesh) and 1.25 Million elements (fine mesh) have been created. These meshes are shown on Figure 3 for the example of a horizontal cut plane which goes through the lower line of the core barrel flow holes.

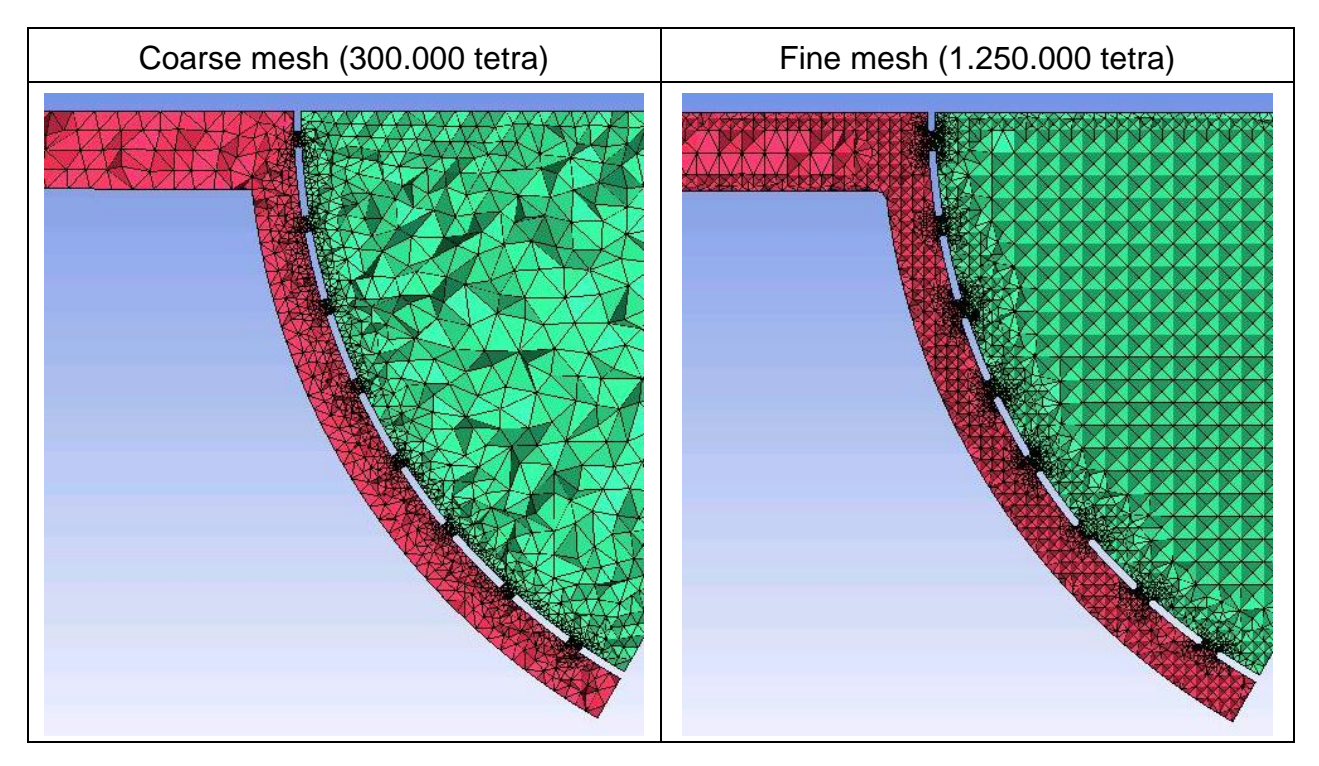


Figure 3 Mesh in a cut plan which goes horizontally through the core barrel flow holes

# 2.4 Thermo-physical properties of Sodium

Liquid Sodium is used as coolant in the MONJU reactor. In the temperature range of interest (380°C to 512°C), the fluid can be treated in first approximation as incompressible.

Table 3 Physical properties of Sodium at 400°C

Quantity	value	unit
Density	858	kg.m <sup>-3</sup> ,
Dynamic viscosity:	2.81*10 <sup>-4</sup>	kg.m <sup>-1</sup> .s <sup>-1</sup> ,
Thermal conductivity:	69.7	W.m <sup>-1</sup> .K <sup>-1</sup> ,
Heat capacity:	1284	J.kg <sup>-1</sup> .K <sup>-1</sup> ,
Volumetric thermal-expansion coefficient:	2.68*10 <sup>-4</sup>	K <sup>-1</sup> .

This simplification allows the application of the Boussinesq hypothesis what means that all physical properties have been treated as temperature independent and buoyancy effects are taken into account only via the gravitational acceleration. The thermo-physical data are given on Table 3 for a reference temperature of 400°C.

## 2.5 Trio\_U code and the numerical scheme

Trio\_U [6] is a thermalhydraulic code for strongly unsteady, low Mach number, turbulent flows. The code is especially designed for industrial CFD calculations on structured and non-structured grids of several tens of millions of nodes. The platform independent code, developed at the CEA-Grenoble, is based on an object oriented, intrinsically parallel approach and is coded in C<sup>++</sup>. The flexible code structure allows the user to choose a suitable discretization method and to combine various appropriate physical models, including different treatments of turbulence. Several convection and time marching schemes as well as a wide range of boundary conditions are available. This flexibility is implemented for massively parallel computing without a significant reduction of the overall performance of the code. The numerical scheme of the calculations presented in this paper is summarised on the Table 4.

Table 4 Numerical scheme used in the Trio\_U calculations

General	Dimension	3D calculation		
	Physical properties	Sodium at 400°C		
		Gravity: $g_z$ =-9.81 m <sup>2</sup> .s <sup>-1</sup>		
	Mesh	Tetrahedral		
	Discretization	P0/P1 for: pressure		
		P1NC for: velocity,		
		temperature,		
		k and ε		
Time scheme		1 <sup>st</sup> order Euler implicit		
Navier-Stokes equation	Convection	muscl		
	Diffusion	Centered		
	Pressure solver	Cholesky		
	Thermal effects	Boussinesq hypothesis		
	Wall law	Logarithmic wall law		
	Turbulence	RANS: Boussinesq approximation		
		with turbulent viscosity $(v_t)$		
Turbulence	Turbulence model	High Reynolds k – ε model		
	$k - \epsilon$ convection	Muscl		
	$k - \varepsilon$ diffusion	Centered		
Thermal equation	Temperature convection	Muscl		
	Temperature diffusion	Centered		
	Wall law	Logarithmic wall law		
	Turbulence	Turbulent Prandtl number Pr		
Mass conservation	Incompressible fluid	Pressure solver (projection method)		
	div(u)=0			

For unstructured, tetrahedral grids, a hybrid « Finite Volume based Finite Element » method (VEF) is applied. This method approximates a continuous problem by a discrete solution in the space of the finite element by maintaining the balance notation of finite volumes. In Trio\_U, the main unknowns as velocity and temperature are located in the centre of the faces of an element (P1NC). This discretization leads to approximately twice as much control volumes for momentum and scalar conservation than present tetrahedrons. The pressure is discretized in both the center (P0) and the vertices (P1) of an element. The resulting staggered mesh arrangement improves the velocity/pressure coupling. An implicit velocity projection method is used to assure the mass conversation [7]. In the solution procedure, a transient is calculated until the main unknowns reach steady state conditions. More detailed information can be found in [6].

# 2.6 Turbulence modelling

Turbulent mixing is treated with the k- $\varepsilon$  model. The high Reynolds form of the model is "appropriate" to fully developed turbulent flows and allows to some extent the presence of buoyancy effects [8]. In the Boussinesq hypothesis framework, the turbulent viscosity is linked to the turbulent kinetic energy  $\varepsilon$  via:

$$v_{t} = C_{\mu} \frac{k^{2}}{\varepsilon}. \tag{5}$$

Conservation equations are written for both the turbulent kinetic energy k and the turbulent dissipation rate  $\epsilon$ .

$$\frac{\partial k}{\partial t} + \overline{u}\nabla k = \nabla \cdot (\frac{V_t}{\sigma_k}\nabla k) - \varepsilon + P + G. \tag{6}$$

$$\frac{\partial \varepsilon}{\partial t} + \overline{u} \nabla \varepsilon = \nabla \cdot \left( \frac{v_t}{\sigma_{\varepsilon}} \nabla \varepsilon \right) - C_{\varepsilon 2} \frac{\varepsilon^2}{k} + C_{\varepsilon 1} P \frac{\varepsilon}{k} + C_{\varepsilon 1} C_{\varepsilon 3} G \frac{\varepsilon}{k}$$
 (7)

The production of turbulence kinetic energy is calculated by

$$P = -\overline{u_i u_j} \frac{\partial \overline{u_i}}{\partial x_j} \qquad \text{with} \qquad -\overline{u_i u_j} = v_t \left( \frac{\partial \overline{u_i}}{\partial x_j} + \frac{\partial \overline{u_j}}{\partial x_i} \right) - \frac{2}{3} k \delta_{ij}$$
 (8)

Buoyancy effects for incompressible flows are treated by

$$G = \frac{V_t}{\Pr} \beta_T g \nabla \overline{T} . \tag{9}$$

The following empirical coefficients (Table 5) are used.

Table 5 Default coefficients of the standard high Reynolds number k-ε model

$C_{\mu}$	$\sigma_k$	$\sigma_{\epsilon}$	$C_{\epsilon 1}$	$C_{\epsilon 2}$	$C_{\varepsilon 3}$	$Pr_t$	$Sc_t$
0.09	1.0	1.3	1.44	1.92	1.0	0.9	0.9

To take into account the effect of thermal stratification, the following assumption is made [8]:

 $C_{\varepsilon^3} = 0$  if G < 0 (stable stratification with reduced buoyancy effects)

 $C_{\varepsilon 3} = 1$  if G > 0 (unstable stratification with full buoyancy effects)

This extension of the standard k-ε model has been tested for Sodium flow by analyzing various natural and mixed convection experiments [9].

# 2.7 Boundary conditions

For each SA outlet, the time depending mass flow rate and temperature are given in the data description report [9] for selected instances during the whole pump trip experiment. Continuous values are interpolated linearly between reported ones. The mass flow rates are converted to velocity inflow boundary conditions by applying on one hand the physical properties of Table 3 and on the other hand the free surface of a SA outlet (11573 mm<sup>2</sup>). A spatially uniform distribution of the temperature and the velocity is assumed for each SA outlet. The turbulent kinetic energy k and its dissipation rate  $\varepsilon$  are predicted from the assembly diameter and a fluctuation velocity which is assumed to be 10% of the mean SA outflow velocity.

All walls are treated as adiabatic walls. Standard logarithmic wall functions (Reichardt [6]) are applied for momentum equations. The two lateral surfaces of the 60° geometry are modelled with the symmetry hypothesis. A pressure outlet condition, associated with free out stream conditions for the velocity and the temperature are used as boundary condition for the outlet nozzle boundary.

## 3. Analysis of the steady state condition before the pump trip experiment

At the beginning of the trip transient, the temperature field and the velocity flow are well established in the Upper Plenum. A first calculation is performed in order to obtain this initial condition. The boundaries conditions for the calculation are the conditions at the beginning of the test [10]. Starting from a reposing ( $\vec{u}$ =0), isothermal flow, the flow field is considered as established in the plenum when all 120 temperature samples placed along the thermocouple plug have reached a stabilized value. At that time, the calculated temperature profile should be close to the temperature profile measured by the thermocouple plug. Three different steady solutions have been achieved which can be distinguished regarding the driving physical process:

- A momentum dominated solution S1
- A buoyancy dominated solution S2
- A mixed convection dominated solution S3

All solutions have a similar reduced Froude Number  $Fr = u/\sqrt{g \cdot \Delta \rho/\rho \cdot d}$  which is in the order of 3.5 (mixed convection). The resulting three different flow patterns and temperature fields are given in Figure 4. A vertical cut plane in a symmetry plan is shown and the temperature profiles along the thermocouple plug are compared. From these temperature profiles it seems not possible to conclude definitively on the flow patterns which have been present during the MONJU experiment. Nevertheless, extensive sensitivity studies on the meshing, on the order of the numerical scheme and on the initialisation of the calculation give some insight on the code behaviour. The effects of the sensitivity studies are summarized in Table 6.

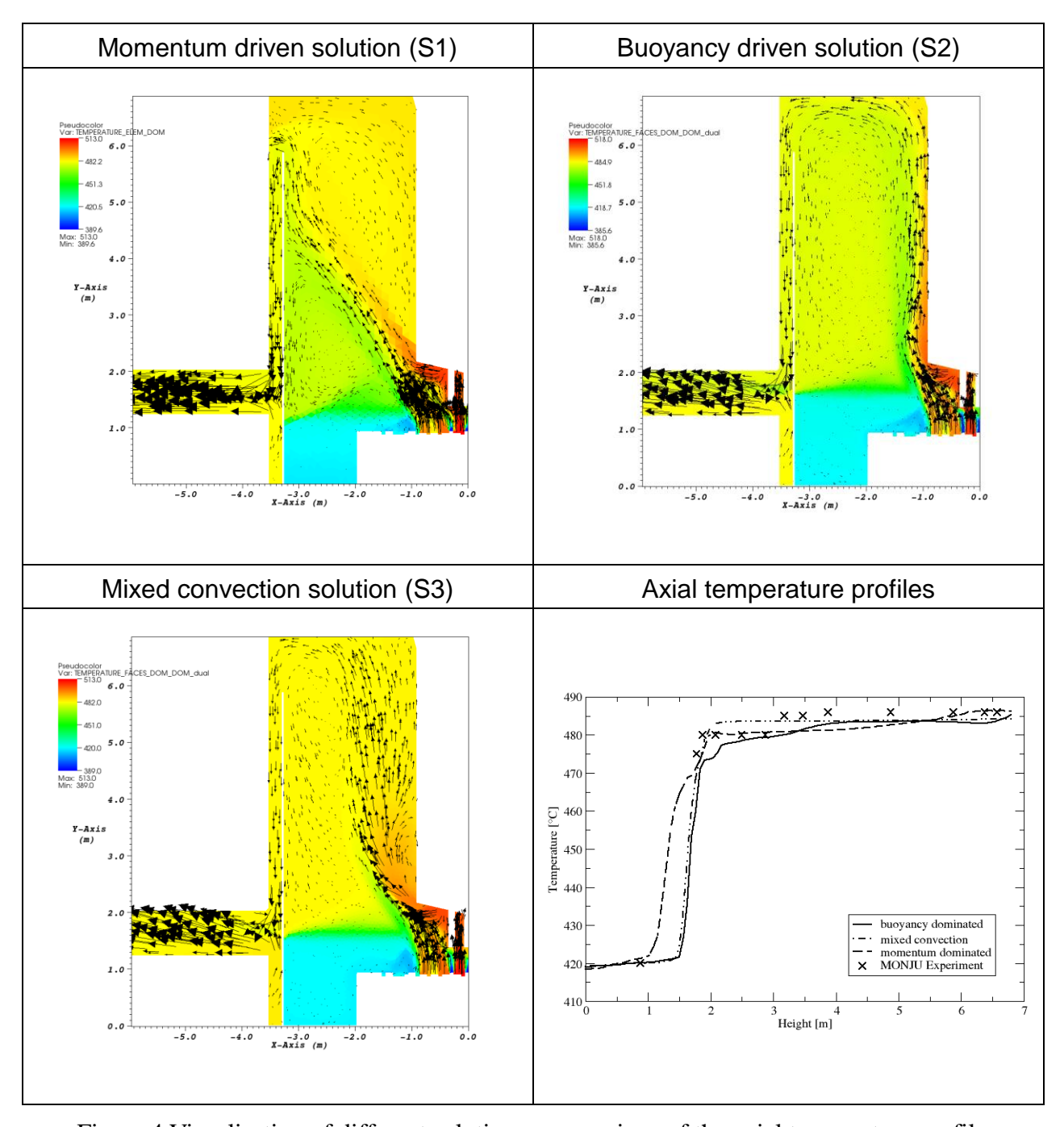


Figure 4 Visualisation of different solutions; comparison of the axial temperature profiles

The following conclusions of the sensitivity calculations can be made:

- A bifurcation into "momentum" and "buoyancy" driven solutions is observed, depending on the mesh refinement and the order of the numerical scheme.
- The momentum driven solution (S1) seems to be attained for the "coarse mesh" and first order convection scheme (initializing with a reposing fluid),
- The buoyancy driven solution (S2) seems to be attained for the "fine mesh" and second order convection schemes (initializing with a reposing fluid),

- Once a stationary solution is achieved (either S1 or S2), this solution can not be altered by changing the numerical scheme and/or the mesh refinement (stable solution).
- The modelling of the UCS has a strong influence on the flow pattern, especially on the width and angle of the jet leaving the UCS; however a real qualification of the modelling is not possible due to the lack of data.

Table 6 Procedures to achieve the different solutions

Initialisation at t=0s	Solution procedure	Solution
Coarse mesh; Reposing flow field at T=418°C	Transient calculation to reach steady state conditions; first order convection scheme: upwind	<b>S</b> 1
Fine mesh; Reposing flow field at T=418°C	Transient calculation to reach steady state conditions; second order convection scheme: muscl	S2
Fine mesh; Reposing flow field at T=513°C	Transient calculation to reach steady state conditions; first order convection scheme: upwind	S2
Fine mesh; Solution S2; UCS is not modelled	Transient calculation to reach steady state conditions; second order convection scheme: muscl	<b>S</b> 3
Fine mesh; Solution S1;	Transient calculation to reach steady state conditions convection schemes: upwind, muscl Time schemes: 1 <sup>st</sup> order explicit; 1 <sup>st</sup> order implicit	<b>S</b> 1
Fine mesh; Solution S2;	Transient calculation to reach steady state conditions convection schemes: upwind, muscl Time schemes: 1 <sup>st</sup> order explicit; 1 <sup>st</sup> order implicit	S2

In order to verify mesh convergence, a simulation on 3.3 million tetrahedral elements has been achieved. Starting from a reposing flow at T=418°C and applying a second order convection scheme (muscl) the buoyancy driven solution S2 has been attained as steady state solution.

The detailed "history" which had led to the flow pattern in the MONJU plant before the pump trip experiment is not known by the author. Assuming the same sensitivity of the flow pattern in the MONJU plant as in the sensitivity calculation, it seems hardly possible to predict clearly and without ambiguity the flow patterns at the beginning of the experiment. Nevertheless, JAEA has estimated from many scaled tests using sodium and water that the momentum driven solutions were close to the actual behaviour. According to JAEA, this assumption is supported by the measured temperature change in the middle part of the plug, 3m and 3.75m above the vessel bottom. However, the momentum driven solution S1 presented in Figure 4 did not reproduce these temperature changes whereas the buoyancy driven solution S2 does roughly.

# 4. Analysis of the pump trip experiment

The analysis of the pump trip transient has shown a fairly well prediction of the thermal stratification formation in the first 10 minutes of the pump trip (see results presented below). This is particularly true for calculations with the "fine" mesh. In the calculation, the stratification disappears after about 15 minutes and a homogeneous temperature distribution is predicted for

the Upper Plenum (not shown in this paper). In the experiment however, the thermal stratification persists for more than one hour.

During the 3<sup>rd</sup> IAEA-RCM meeting, an underestimation of the flow passing through the core barrel holes has been identified as a potential source of uncertainty regarding long term stratification formation. For the exact form of the holes is not known to date, the impact of the two extreme hole-forms on the stratification formation was analysed; sharp edged holes and rounded holes (fillet) which have the same minimum cross section as the sharp edged holes.

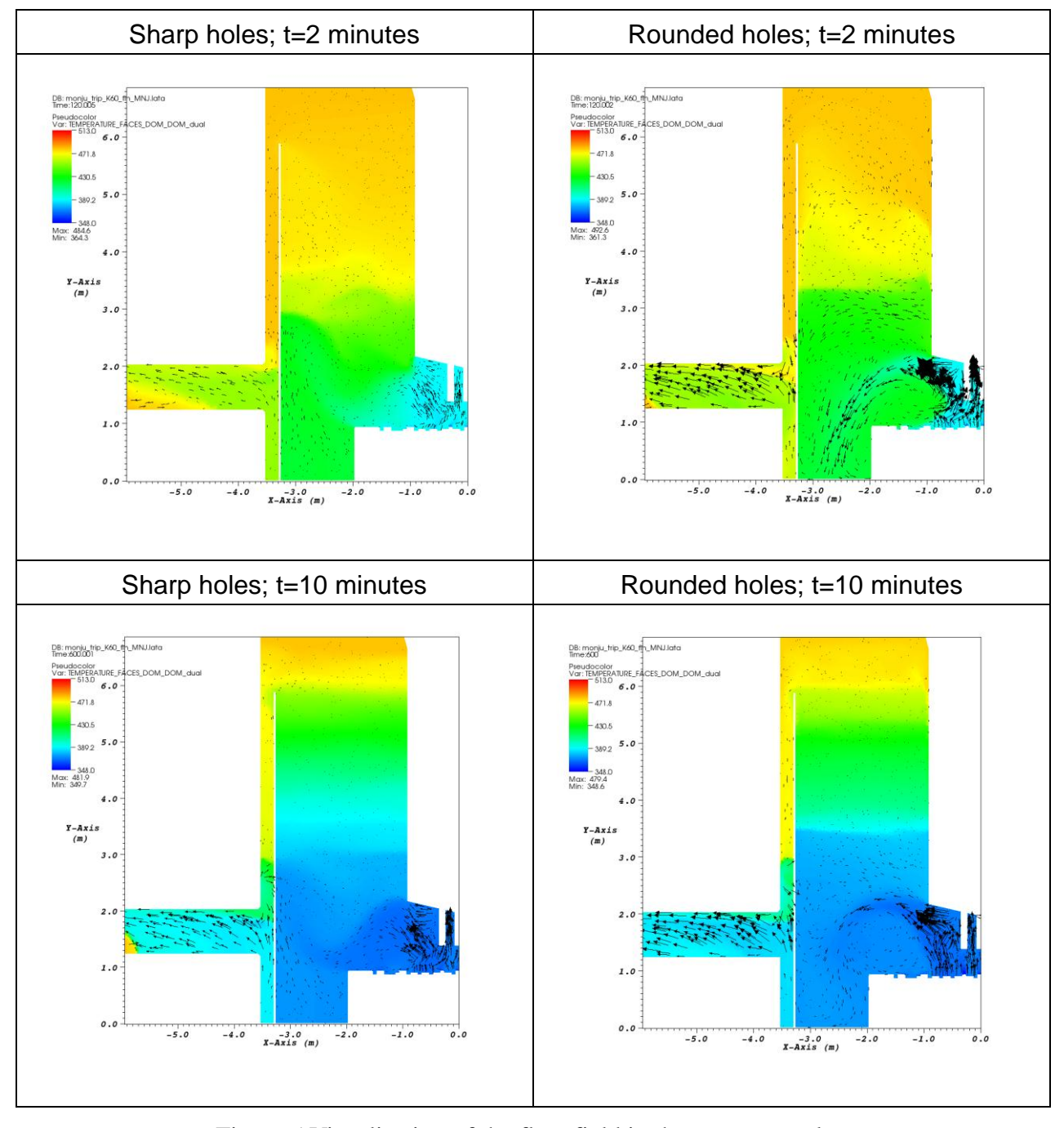


Figure 5 Visualisation of the flow field in the symmetry plane

Figure 5 shows the thermal stratification in the symmetry plane, 2 minutes and 10 minutes after the beginning of the pump trip (initialising with solution S2). The "fine mesh" and 2<sup>nd</sup> order discretization schemes are applied. The overall flow patterns of the two calculations look rather different (instantaneous conditions are visualised). Nevertheless, the resulting thermal stratifications seem not being influenced significantly by the flow field. This can be seen from the axial temperature profiles along the thermocouple plug shown on Figure 6. The effect of the flow holes at about 3m and 3.75m on the calculated temperature profiles is visible. Such an effect of the flow holes on the temperature stratification seems not being present in the measurement.

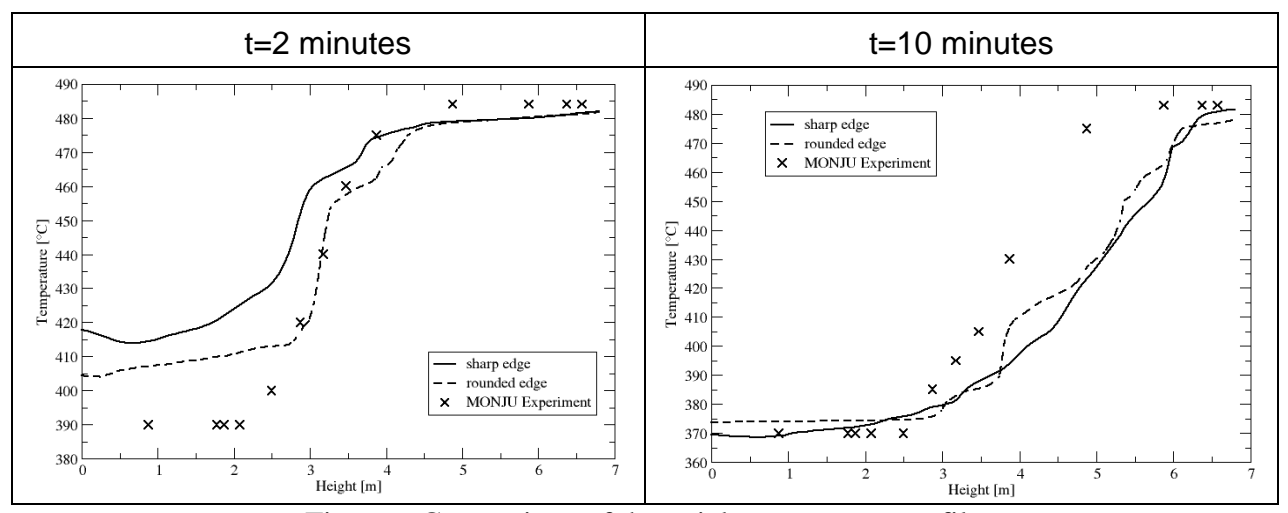


Figure 6 Comparison of the axial temperature profiles

Thus, a final decision on the potential influence of the flow holes on the thermal stratification cannot be made by these calculations. Nevertheless, in the presented calculation, the form of the holes does not explain the overestimation of the upward movement of the stratification front.

#### 5. Conclusion

In the framework of an IAEA CRP, benchmark analyses of sodium convection in the Upper Plenum of the MONJU reactor vessel has been performed at CEA-Grenoble by using the CFD code Trio\_U. Azimuthally, 1/6 of the MONJU Upper Plenum has been taken into account in the modeling. This reduced domain was discretized in up to 3.3 Million tetrahedral elements. A high Reynolds number turbulence model (k-ε) was used to account for turbulent mixing with additional terms for treating buoyancy effects.

For the steady state initial condition of the pump trip transient, a bifurcation of the solution is observed, depending on the mesh refinement and the order of the numerical scheme. Starting from a reposing fluid, the momentum driven solution was attained only for the "coarse mesh" and first order convection scheme whereas the buoyancy driven solution was attained for the "fine mesh" and second order convection schemes. The experimentally found temperature stratification seems not being a good indicator to distinguish the flow fields of the two solutions. For a more profound understanding, further numerical analysis is necessary. This concerns the solution procedure (iterative methods as SIMPLE instead of transient methods as presented) as well as the use of more sophisticated turbulence modelling approaches.

The pump trip experiment has shown the formation of a thermal stratification within the plenum. The calculations on the "fine mesh" predict well the stratification formation in the first 10 minutes of the pump trip. In the experiment, the stratification persists for more than one hour whereas all calculations of Trio\_U have shown a homogenization of the temperature in the plenum after about 15 to 20 minutes (significant overestimation of the internal mixing).

#### 6. References

- [1] S. Yoshikawa et al.: "Data description for Numerical Analyses of Sodium Natural Convection in the Upper Plenum of the MONJU Reactor Vessel". Presented for: First Research Coordination Meeting (RCM) of the IAEA Coordinated Research Project (CRP) on "Benchmark Analyses of Sodium Natural Convection in the Upper Plenum of the MONJU Reactor Vessel" 22-24 September 2008, IAEA Headquarters, Vienna
- [2] S. Yoshikawa et al.: "PDF file: Measurable Geometry File". Presented for: First (Kickoff) Research Coordination Meeting (RCM) of the IAEA Coordinated Research Project (CRP) on "Benchmark Analyses of Sodium Natural Convection in the Upper Plenum of the MONJU Reactor Vessel" 22-24 September 2008, IAEA Headquarters, Vienna
- [3] T. Sofu, J. Thomas and T. Fanning: "Analysis of Thermal Stratification in the Upper Plenum of the MONJU Reactor Vessel using a Simplified Model", Second Research Coordination Meeting IAEA Coordinated Research Project on "Benchmark Analysis of MONJU Natural Convection", 12-14 October 2009, Marcoule, France
- [4] V. Blind, U. Bieder and T. Sofu: "Benchmark Analysis of Sodium Natural Convection in the Upper Plenum of the MONJU Reactor Vessel: Preparation of a simplified model for the Upper Core Structures", DEN/CAD/DER/SSTH/LMDL/NT/2009-105
- [5] Idel'Cik I.E.: "Mémento des pertes de charges: Coefficient de pertes de charge singulières et de perte de charge par frottemnt". Direction des études et recherches d'Electricité de France (EDF), 1986
- [6] Trio\_U: http://www-trio-u.cea.fr
- [7] Guermond J.-L., Quartapelle L.: "On the Stability and Convergence of Projection Methods Based on Pressure Poisson Equation" Int. J. Numer. Meth. Fluids **26**: 1039–1053 (1998)
- [8] Viollet P-L.: "Mécanique des fluides à masse volumique variable. Aérodynamique, thermohydraulique, écoulements stratifiés, transferts de chaleur". Presses de l'école nationale des Ponts et chaussées, 1997
- [9] D. Tenchine: "Some thermalhydraulic challenges in sodium cooled fast reactors". Nuclear Engineering and Design 240 (2010) 1195–1217
- [10] S. Yoshikawa et al.: "Complementary descriptions for detailed boundary conditions" Presented for: First (Kick-off) Research Coordination Meeting (RCM) of the IAEA Coordinated Research Project (CRP) on "Benchmark Analyses of Sodium Natural Convection in the Upper Plenum of the MONJU Reactor Vessel" 22-24 September 2008, IAEA Headquarters, Vienna